

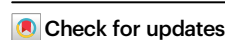


Developing an alternative medium for in-space biomanufacturing

Received: 26 June 2024

Accepted: 8 January 2025

Published online: 16 January 2025



Hakyung Lee¹, Jinjin Diao¹✉, Yuxin Tian^{1,2}, Richa Guleria³, Eunseo Lee¹, Alexandra Smith⁴, Millie Savage⁵, Daniel Yeh⁴, Luke Roberson⁶, Mark Blenner^{1,3}, Yinjie J. Tang¹✉ & Tae Seok Moon^{1,2}✉

In-space biomanufacturing provides a sustainable solution to facilitate long-term, self-sufficient human habitation in extraterrestrial environments. However, its dependence on Earth-supplied feedstocks renders in-space biomanufacturing economically nonviable. Here, we develop a process termed alternative feedstock-driven in-situ biomanufacturing (AF-ISM) to alleviate dependence on Earth-based resupply of feedstocks. Specifically, we investigate three alternative feedstocks (AF)—Martian and Lunar regolith, post-consumer polyethylene terephthalate, and fecal waste—to develop an alternative medium for lycopene production using *Rhodococcus jostii* PET strain S6 (RPET S6). Our results show that RPET S6 could directly utilize regolith simulant particles as mineral replacements, while the addition of anaerobically pretreated fecal waste synergistically supported its cell growth. Additionally, lycopene production using AF under microgravity conditions achieved levels comparable to those on Earth. Furthermore, an economic analysis shows significant lycopene production cost reductions using AF-ISM versus conventional methods. Overall, this work highlights the viability of AF-ISM for in-space biomanufacturing.

Space exploration plays a pivotal role in expanding our understanding of the cosmos, enabling humans to create new opportunities and inspire the world through discovery. Notably, the challenges of space exploration often serve as a catalyst for innovation, driving the development of cutting-edge technologies that find applications across various industries and ultimately benefit society as a whole. So far, the enthusiasm for space exploration, particularly the long-duration human space ventures (e.g., returning to the Moon, traveling to Mars, and visiting asteroids), has significantly intensified¹. To realize such grand visions, intensive abiotic approaches for extending human presence in space have emerged^{2–5}.

With the advancement of synthetic biology, microbial biomanufacturing holds excellent potential to establish alternative supply chains for the cost-effective production of consumable and durable

goods⁶. This capability, coupled with the microbial adaptive plasticity⁷, plays an integral role in developing efficient and sustainable life support systems. For instance, microorganisms can self-replicate and self-sustain with only occasional monitoring and maintenance, reducing energy demand compared to physicochemical approaches when applied for manufacturing purposes⁸. Recognition of these advantages has prompted attempts to produce pharmaceuticals onboard the International Space Station (ISS). Results demonstrated that under the condition of weightlessness, microbial production of antibiotics was significantly increased^{9,10}. Although biotechnologies hold great promise to establish a sustainable process for producing consumables with minimal input, an actionable roadmap for deploying microbial biomanufacturing to develop self-sufficient life support systems for long-duration and deep space exploration remains largely unexplored^{11,12}.

¹Washington University in St. Louis, Saint Louis, MO, USA. ²Synthetic Biology Group, J. Craig Venter Institute, La Jolla, CA, USA. ³University of Delaware, Newark, DE, USA. ⁴University of South Florida, Tampa, FL, USA. ⁵Lincoln University of Missouri, Jefferson City, MO, USA. ⁶National Aeronautics and Space Administration, John F. Kennedy Space Center, Merritt Island, FL, USA. ✉e-mail: j.diao@wustl.edu; yinjie.tang@wustl.edu; tsmoon7@gmail.com

Space exploration is costly when viewed solely economically, with returns on investment primarily measured by scientific output². In situ resource utilization (ISRU) can significantly minimize the dependence on initial launch cargo and resupply from Earth, contributing to the establishment of financially sustainable space exploration programs^{7,12–15}. It refers to generating consumables to support human activities using materials found locally on the planetary bodies¹⁶. For example, efforts have been made to produce Mars-specific rocket propellant, 2,3-butanediol (2,3-BDO), from CO₂, sunlight, and water on Mars via a biotechnology-enabled in-situ resource utilization (bio-ISRU) strategy¹⁷. Regolith-driven ISRU was developed to extract H₂O and O₂ for life support and/or H₂ and O₂ for fuel and propellant from planetary regolith^{3,18}. Moreover, elements derived from planetary regolith have also been developed into biological feedstocks for feeding plants^{19,20}, demonstrating the promising feasibility of utilizing local materials to support in-space microbial biomanufacturing.

Notably, beyond its promising economic feasibility, in-space microbial biomanufacturing offers the additional advantage of utilizing waste streams generated by crew members (referred to as loop-closure, LC), which is a critical aspect of achieving the self-sustainability of mission operations. Furthermore, this process can effectively address the ethical concerns associated with space waste generation, particularly in long-distance missions²¹. Numerous initiatives are underway to develop high-efficiency systems for recycling or upcycling biological wastes, including CO₂, food waste, and black, gray, and yellow water^{22,23}. Plastics—known for their high strength and durability—are widely used in space exploration missions, ranging from food packaging to components of spacecraft and spacesuits²⁴. It is estimated that each crew member generates 0.34 kg of plastic waste per day²⁵, posing a significant challenge for plastic waste management during human space exploration. Consequently, there is an urgent need to develop sustainable and effective strategies for managing plastic waste generated during space exploration. Plastic bio-upcycling, which combines chemical catalysis to convert plastic waste into microbially metabolizable feedstocks with their subsequent biological catalysis to produce value-added products, has been developed in terrestrial environments, offering an attractive path toward a fully circular plastic economy^{26–34}. Even though researchers at the UK Center for Astrobiology are exploring if the microbial degradation of plastics could be leveraged for plastic recycling in space²¹, the development of plastics into feedstocks for in-space microbial biomanufacturing remains unexplored.

Another major concern for human space exploration is that, in extraterrestrial environments, astronauts often experience health problems, such as bone mineral density and weight loss, muscle atrophy, and reduced immune function^{35–37}. Consequently, maintaining healthy diets for astronauts is crucial for supporting human endeavors. To this end, NASA has been developing durable foods with additional nutrients to support astronaut's health. For instance, lycopene—a bioactive compound beneficial for bone health and cancer prevention—has been selected as a nutritional additive in several ISS food candidates³⁸. Currently, for missions aboard ISS, sufficient food and nutrients are available from initial launch cargo or regular resupplies from Earth³⁹. However, for long-term human space ventures, such as visiting asteroids and traveling to and inhabiting Mars, the logistic resupply of life-supporting goods (e.g., nutrients, pharmaceuticals, and biomaterials) becomes increasingly challenging due to the vast interplanetary distances⁴⁰. Although an engineered yeast platform has been proposed as a versatile alternative for the cost-effective production of food and nutrients off-world⁸, this process still relies on the resupply of essential components from Earth, including carbon sources, macronutrients, and trace elements. This dependency compromises its effectiveness in supporting self-sufficient human travel and habitation through the solar system.

In this study, to address these challenges, we developed a process termed alternative feedstock-driven in-situ biomanufacturing (AF-ISM)

to produce consumables from alternative feedstocks (i.e., plastic waste, fecal waste, and regolith), thereby validating the feasibility of deploying biomanufacturing for self-sufficient life support systems (Fig. 1). This process employs *Rhodococcus jostii* PET strain S6 (hereafter RPET S6)²⁶—a lycopene-producing specialist capable of using poly(ethylene terephthalate) (PET) hydrolysate as the sole carbon source for sustainable lycopene production—as the microbial platform. We initially tested Lunar or Martian regolith as a mineral source in the growth medium for RPET S6 (due to limited access to actual regolith, their corresponding simulants were utilized throughout this study). Next, we optimized the nutrient concentration of permeate derived from anaerobically pretreated fecal waste to provide nitrogen and phosphorus for supporting RPET S6 proliferation. Finally, we validated AF-ISM for sustainable lycopene production under the simulated microgravity condition, using a completely alternative medium in which conventional components were all replaced with alternative feedstocks. Our results demonstrated that the lycopene production level from the AF-ISM process was almost identical to that achieved on Earth. Furthermore, the production cost is significantly lower compared with conventional methods. Overall, this study highlights the great potential of AF-ISM as an emerging technology to harness in-situ resources and waste streams for sustainable production of nutritional additives (i.e., lycopene). Additionally, this bioprocess can be integrated with other enabling technologies to develop long-term, self-sufficient life support systems, which are crucial for establishing settlements on the Moon and Mars, as well as enabling future deep space exploration.

Results

Testing the acidified Lunar and Martian regolith simulants as alternative mineral sources

Given the exposure to harsh environments, the microbial chassis selected for off-world biomanufacturing must have high adaptability to various stress conditions. Notably, *Rhodococcus* is distinguished by its remarkable catabolic versatility and resistance to stressful environmental conditions, making it a widely studied microbial chassis for multiple applications, such as steroid transformation, lignin valorization, petroleum desulfurization, and oleochemical bioproduction^{41–46}. We previously identified *Rhodococcus jostii* PET (RPET) that can directly use PET hydrolysate as a sole carbon source, enabling its development into a robust microbial platform (e.g., RPET S6) for upcycling of PET waste to lycopene via synthetic biology²⁶. Therefore, we selected and tested the corresponding RPET strain as a candidate for potential applications in off-world biomanufacturing.

The financial and ethical concerns of space exploration highlight the significance of ISRU in in-space microbial biomanufacturing technologies for developing long-term and self-sufficient life support systems. Minerals are essential for microbes to support their intracellular metabolism⁴⁷. In this study, to minimize the dependence on Earth-sourced minerals for in-space microbial biomanufacturing, we intended to test Lunar or Martian regolith as a mineral source for supporting RPET S6 cell growth. Due to limited access to actual regolith, we used the corresponding simulants—Lunar physical and chemical regolith simulant and Martian regolith simulant—throughout this study. The Lunar physical simulant, Black Point One (BP-1), was chosen because it is the most representative Lunar regolith simulant, with physical properties similar to natural Lunar regolith. The Lunar chemical simulant, Johnson Space Center One (JSC-1/1A), was selected for its chemical composition, which mirrors the soil from the Maria geological terrain of the Moon⁴⁸. Mars Global Simulant (MGS-1) was used as it serves as a mineralogical standard for basaltic soils on Mars, developed based on quantitative mineral data from the MSL Curiosity rover⁴⁹. Before testing their effectiveness in supporting microbial growth, we first characterized the chemical compositions of each regolith simulant. Our results indicated that the chemical

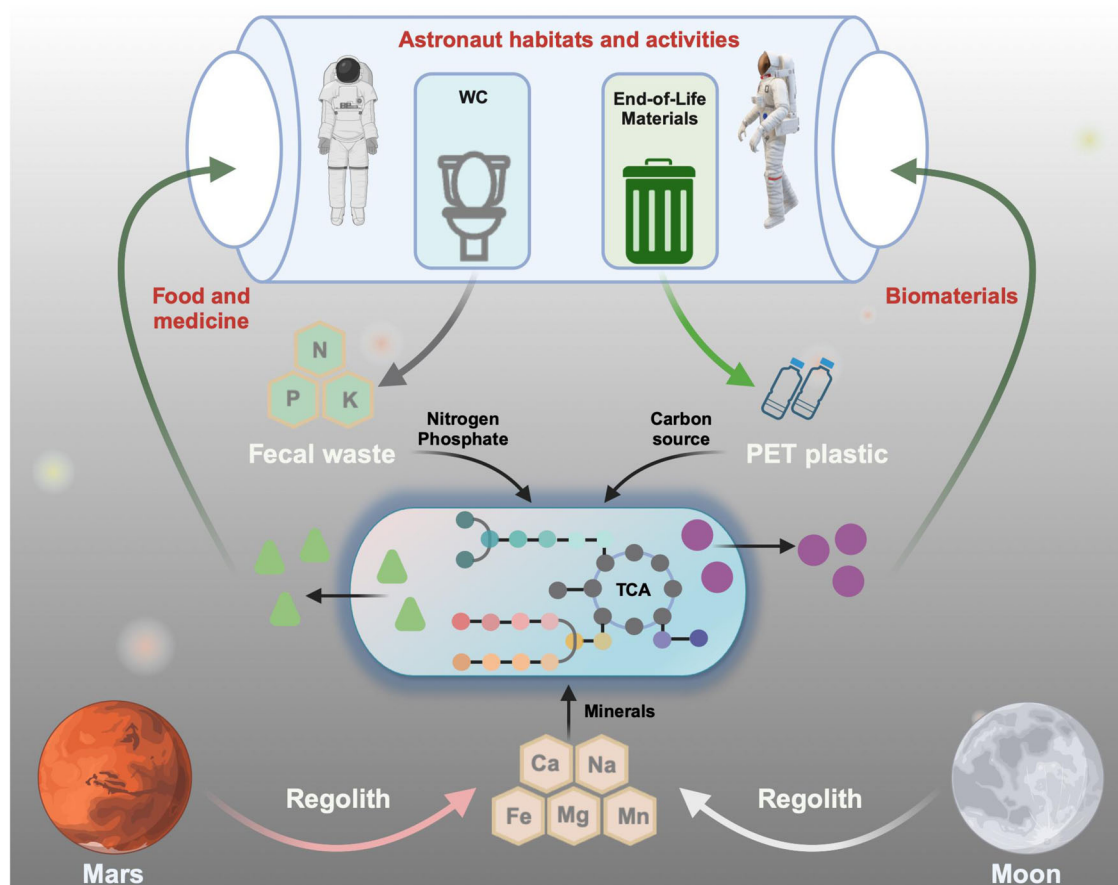


Fig. 1 | Conceptual diagram of the alternative feedstock-driven in-situ biomanufacturing (AF-ISM) for sustainable life support systems in space. In this process, in-situ resources (e.g., Lunar and Martian regolith), end-of-life materials (e.g., PET plastic), and human waste (e.g., astronaut fecal waste) can be converted

into metabolizable substrates to feed microbial chassis for producing consumables such as food, medicine, and other biomaterials to sustain life support systems. This figure was created with BioRender.com.

compositions of Lunar and Martian regolith simulants are identical, but the content of individual elements varied. Interestingly, a comparison between the leachates from Lunar physical and chemical regolith simulants showed that the chemical regolith simulant contained higher or similar concentrations of all elements except calcium (Supplementary Table 1).

To assess the potential toxicity of the acidified regolith simulant, we prepared minimal media with varying concentrations of the simulant and tested its effects on RPET S6 cell growth. Specifically, the media contained regular levels of nitrogen (N) and phosphorus (P), equimolar mixtures of terephthalic acid (TPA) disodium salt and ethylene glycol (EG) as carbon sources, and varying concentrations of the acidified regolith simulant solutions (ranging from 0.5 g/L to 8.0 g/L). As expected, cell growth defect was observed when no minerals were supplied in the minimal medium (Fig. 2a), suggesting the essential role of minerals in supporting microbial cell growth⁴⁷. Notably, our results showed that RPET S6 was sensitive to the acidified Lunar physical regolith simulant, with severe cell growth inhibition observed at concentrations exceeding 1.0 g/L. By contrast, no significant inhibition was observed with the acidified Lunar chemical regolith simulant or Martian regolith simulant until their concentrations increased to 4.0 g/L (Fig. 2a). Additionally, the inductively coupled plasma (ICP) and ion chromatography analyses revealed significant decrease in magnesium (Mg), calcium (Ca), iron (Fe), and manganese (Mn) concentrations after cultivation, confirming the successful uptake of regolith simulant-derived minerals by RPET S6 (Supplementary Table 2).

Given the limited resources during space exploration, we reduced the usage of N and P for growing RPET S6. Each acidified regolith simulant was provided at its optimal concentration in the minimal medium with identical levels of carbon source while varying the concentrations of N and P. Our results demonstrated that reducing N and P concentrations to half of those did not result in cell growth deficiencies (Fig. 2b–d). However, when N and P were reduced to 0.1-fold of the levels in the regular medium, significant cell growth deficiency was observed, particularly severe when using the acidified Martian regolith simulant as the mineral source (Fig. 2b–d). Taken together, our results confirmed that both Lunar and Martian regolith could be used as mineral sources to support microbial cell growth, adhering to the principle of ISRU.

Developing regolith simulant particles as a mineral source

In contrast to the utilization of acidified regolith, it would be more economical to use regolith particles to sustain microbial proliferation directly. In the minimal medium supplied with all nutrients except trace minerals, our results revealed that RPET S6 could use either Lunar physical or Martian regolith simulant particles with nearly identical cell growth observed when the particle concentrations were kept below 5.0 g/L (Supplementary Fig. 1). However, a significant inhibitory effect was detected when the regolith concentrations are at or exceeded 10.0 g/L (Supplementary Fig. 1). Subsequently, we tested RPET S6 in the minimal medium supplied with mimicked PET hydrolysate as a carbon source, regolith simulant particles as a mineral source, and varying concentrations of N and P. Interestingly, a

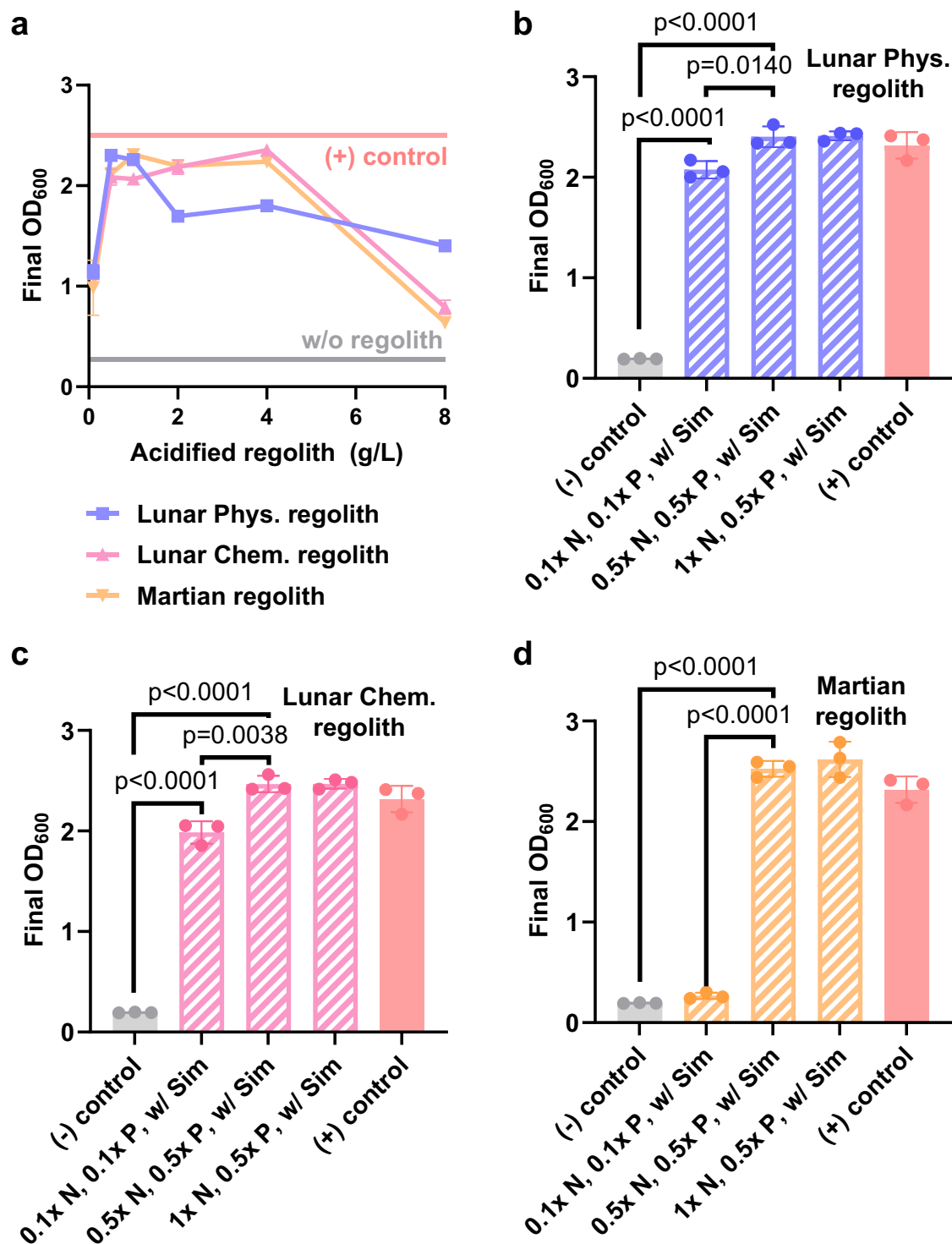
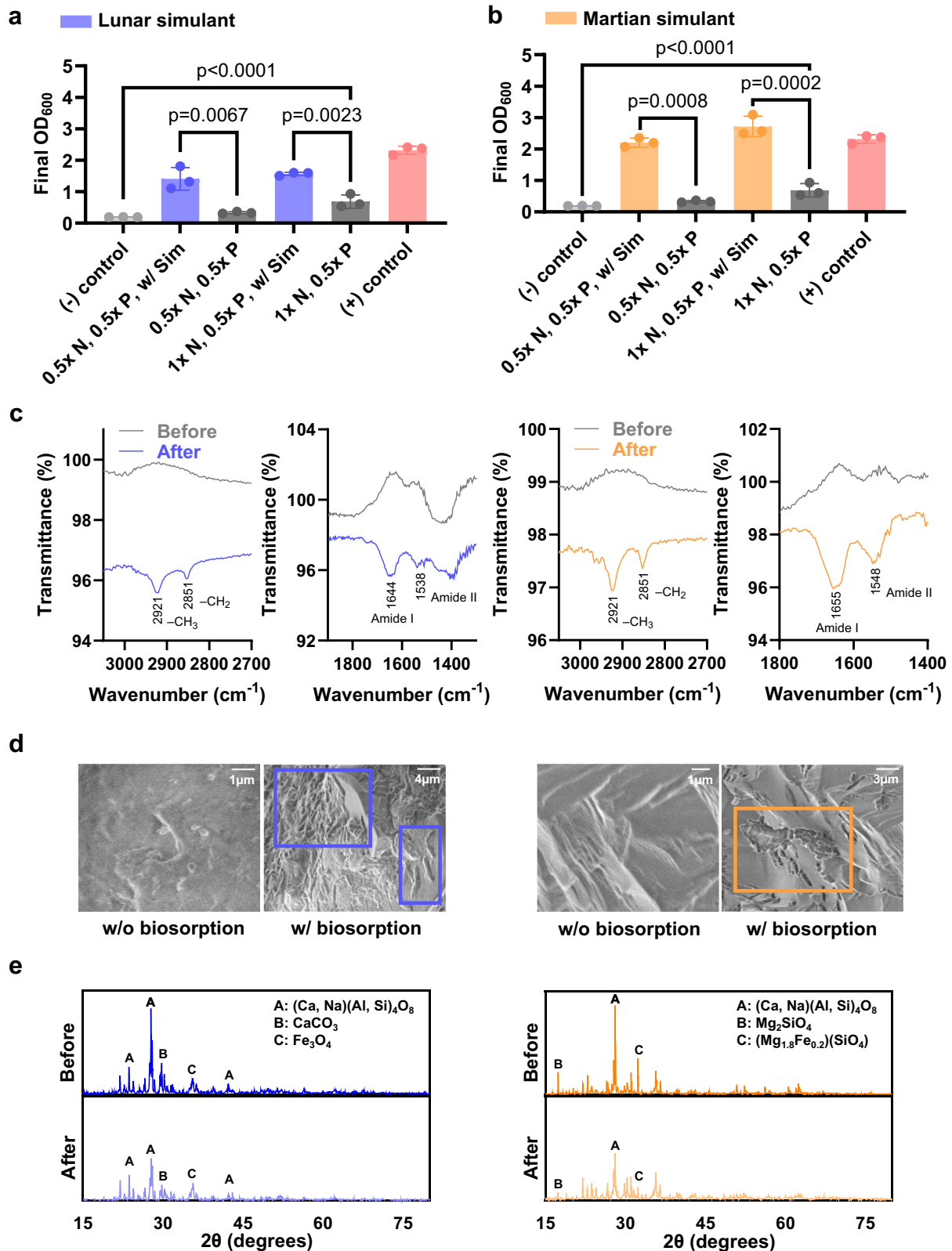


Fig. 2 | Acidified regolith simulant utilization by RPET. a Evaluating the toxicity of acidified Lunar physical (Phys.) and chemical (Chem.) regolith simulant, and Martian regolith simulant (note: error bars of some data points were too small to be shown). RPET S6 was inoculated into the minimal medium with identical nitrogen, phosphorus, and carbon sources and varying concentrations of acidified regolith simulants (ranging from 0.5 g/L to 8.0 g/L). **b–d** Minimizing N and P levels in the minimal medium when using either acidified Lunar physical regolith simulant (**b**), Lunar chemical regolith simulant (**c**), or Martian regolith simulant (**d**) as a mineral source. RPET S6 cultivated in the minimal medium without acidified regolith

simulant represents negative control ((-) control), while cultivation in regular minimal medium represents the positive control ((+) control). The variations in the changes of final cell density (OD₆₀₀) were analyzed by using an unpaired two-tailed *t*-test. The 95% confidence interval for the difference between means of 0.5× N, 0.5× P w/ Sim, with regolith simulant; w/o Sim, without regolith simulant. Source data are provided as a Source Data file.



moderate decrease in cell growth was observed when RPET S6 was cultivated in the medium supplemented with 1.0 g/L Lunar regolith simulant particles and reduced N and P sources (Fig. 3a). In contrast, no inhibition was observed with Martian regolith simulant particles (Fig. 3b).

Given the significant cell growth, we next aimed to uncover the underlying molecular mechanism by which RPET directly utilizes

regolith simulant particles to support its growth. Even though significant mineral leaching from regolith simulant particles was observed in the no-inoculation control medium, certain elements were absent under the specific conditions (i.e., no Mg, K, or Mn leached from the Lunar regolith simulant, and no Mg from the Martian regolith simulant) (Supplementary Table 3). This suggested that mineral absorption during RPET S6 cultivation may result from a combinatorial

Fig. 3 | Using regolith simulant particles as a mineral source for RPET cell growth. **a, b** The minimum levels of nitrogen and phosphorus sources in the minimal medium were determined using either 1g/L of Lunar (**a**) or Martian (**b**) regolith simulant particle as the mineral source. RPET Strain S6 cultivated in the minimal medium without regolith simulant represents the negative control (–) control, while cultivation in a regular minimal medium represents the positive control (+) control. In all conditions, mimicked PET hydrolysate was supplied as a carbon source. The variations in the changes of final cell density (OD_{600}) were analyzed by using an unpaired two-tailed *t*-test. The 95% confidence interval for the difference between means of 1x N, 0.5x P w/ Sim, and negative controls for Lunar and Martian regolith simulants are 1.29 to 1.46 and 2.01 to 3.04, respectively. All

values represent the mean of triplicate cultures ($N=3$), with error bars depicting the standard deviation from that mean. Abbreviations: w/ Sim, with regolith simulant; w/o Sim, without regolith simulant. **c** Fourier-transform infrared spectroscopy analysis to compare the chemical bond changes on the surface of the regolith particles (left panel, Lunar regolith; right panel, Martian regolith). **d** Comparing the surface changes of the regolith particles before and after RPET cell growth through Scanning Electron Microscopy analysis (left panel, Lunar regolith; right panel, Martian regolith). Images are representative of $N=3$ independent experiments. **e** XRD analysis to compare the crystalline structure change of the regolith particles before and after RPET cell growth (left panel, Lunar regolith; right panel, Martian regolith). Source data are provided as a Source Data file.

process. Notably, bioleaching—the interaction between minerals and microbes facilitated by the flow of energy and exchange of matters—affects the dissolution, transformation, and formation of minerals⁴⁷, a mechanism utilized by microbes to extract elements from soil to support their growth^{50,51}. Therefore, we hypothesized that the restored cell growth in the minimal medium with regolith simulant particles as a mineral source could also be attributed to the biological weathering process. To validate this hypothesis, Fourier Transform-Infrared (FT-IR) Spectroscopy analysis was applied to examine the bonding structure changes on the regolith simulant particle surface before and after RPET S6 cultivation⁵². As shown in Fig. 3c, various characteristic peaks were observed after cell cultivation regardless of the regolith simulant type. Among them, the new peak appeared at 2900–2850 cm^{-1} , corresponding to the lipids stretching of $-CH_3$ and $-CH_2$ vibration, indicating the presence of lipids on the surface of the particles⁵³. Additionally, the absorption peaks at 1650 and 1550 cm^{-1} can be assigned to the amide I and amide II bands, respectively⁵³. The amide I band is attributed to the stretching of protein-related amide $C=O$, while the amide II band is ascribed to the bending of amide $N-H$ ⁵⁴. These results demonstrated that RPET S6 could secrete protein-type extracellular polymeric substances on particle surfaces.

Moreover, Scanning Electron Microscopy (SEM) revealed that RPET S6 cells aggregated on the surface of the ore during cultivation (Fig. 3d), facilitating chemical element leaching from regolith particles. The X-ray Diffraction (XRD) analysis further confirmed the crystallinity changes of the particles by consuming the chemical elements. Our results showed that, after cultivation, in the $(Ca, Na)(Al, Si)_4O_8$ content, both Lunar and Martian regolith simulant particles exhibited signal intensity decreases of 52% and 47%, respectively (Fig. 3e). Moreover, $CaCO_3$ consumption was only detected in Lunar regolith simulant, while Mg_2SiO_4 and $Mg_{1.8}Fe_{0.2}SiO_4$ consumption was detected in Martian regolith simulant (Fig. 3e).

Producing lycopene in the semi-alternative medium

After validating the feasibility of using regolith simulant particles as a mineral source for RPET S6 growth, we sought to produce lycopene in the semi-alternative medium, which consists of mimicked PET hydrolysate as a carbon source, regolith simulant particles as a mineral source, and regular N and P sources. Although the cell growth of RPET S6 was inhibited when cultivated in the semi-alternative medium with Lunar physical regolith simulant (Fig. 4a), lycopene production was nearly identical to that of the positive control (Fig. 4b). For Martian regolith, RPET S6 demonstrated comparable cell growth cultivated in either the semi-alternative medium or the regular medium (Fig. 4a). Interestingly, however, the lycopene production was enhanced in Martian regolith-based semi-alternative medium (Fig. 4b).

To exclude the effect of the particle itself, we tested the lycopene production in RPET S6 when cultivated in the minimal medium supplied with acidified regolith simulants as a mineral source. Strain growth in the semi-alternative medium, with either acidified Lunar physical regolith simulant or Martian regolith simulant, was almost comparable to that of the positive control (Fig. 4c). Notably, the subsequent lycopene production assay showed that using acidified

regolith simulant as the mineral source could significantly improve lycopene production compared to the positive control. Additionally, no apparent difference in lycopene production was observed between the two acidified regolith simulants (Fig. 4d).

Developing a complete AF medium for lycopene production

Inefficient human waste management poses an enormous challenge, particularly in long-duration space exploration²¹. Currently, aboard ISS, human waste is ejected from the station to burn up in the Earth's atmosphere after being completely stabilized and dried⁵⁵. This method is not feasible as missions expand. To address the sustainability concerns, we wanted to test the feasibility of utilizing treated human fecal waste as an alternative feedstock for in-space microbial biomanufacturing, as it contains essential nutrients, such as N and P, for microbes. Previously, an anaerobic membrane bioreactor (AnMBR) was developed in collaboration between the University of South Florida (USF) and the Kennedy Space Center (KSC) to treat and recover resources from organic wastes (Fig. 5a), serving as a bioregenerative life support system for early Lunar and Martian base habitats⁵⁶. This prototype, called the Organic Processor Assembly (OPA), was operated for 436 days at USF, processing progressively higher solids inputs (increasing from 1% to 3% and 5%), and included two successful dormancy periods—lasting 54 and 147 days—to evaluate the system's stability and reliability⁵⁶. Moreover, in accordance with the Life Support Baseline Values and Assumptions Document (BVAD)⁵⁷, about 2.5 L human waste per day (calculated based on a nominal crew size of four healthy members)—equivalent to 0.132 kg/CM-day of fecal waste plus 0.5 kg/CM-day of flush water—can be completely processed by the OPA, yielding 2.5 L/day of effluent (permeate). Due to the safety and handling concerns of testing actual human fecal waste, simulated or animal waste is recommended for validating the proof-of-concept under lab conditions⁵⁸. Consequently, in our study, canine waste was chosen as a substitute for human fecal waste. Following AnMBR treatment, compositional analysis of the resulting permeate revealed high concentrations of N and P, reaching up to approximately 392 mg/L and 54 mg/L, respectively (Fig. 5b). Meanwhile, the existence of metal ions (i.e., Na^+ , K^+ , Mg^{2+} , and Ca^{2+}) and even some unknown organic carbon sources could also benefit microbial cell growth (Fig. 5b).

We intended to utilize this permeate as a nutrient substitution, specifically for N and P, to develop a complete AF medium. In an effort to overcome the potential toxicity of the permeate to RPET S6, we first tested its cell growth in the media supplemented with permeate at various dilution factors (0, 0.2, 0.4, 0.6, 0.8, 1.0-fold). Our results showed that RPET S6 exhibited no significant cell growth when cultivated in the medium supplemented with only equimolar mixtures of TPA and EG as the carbon source, while the addition of 0.2-fold diluted permeate restored cell growth, emphasizing the essential role of nutrients in the permeate in supporting the metabolism of RPET S6 (Supplementary Fig. 2). Intriguingly, severe cell growth inhibition was observed in RPET S6 when the permeate dilution factor exceeded 0.4, possibly due to the toxicity of nitrite present in the permeate (Fig. 5b).

A 'synergistic effect' in a microbial growth medium usually occurs when components interact to enhance microbial growth beyond what

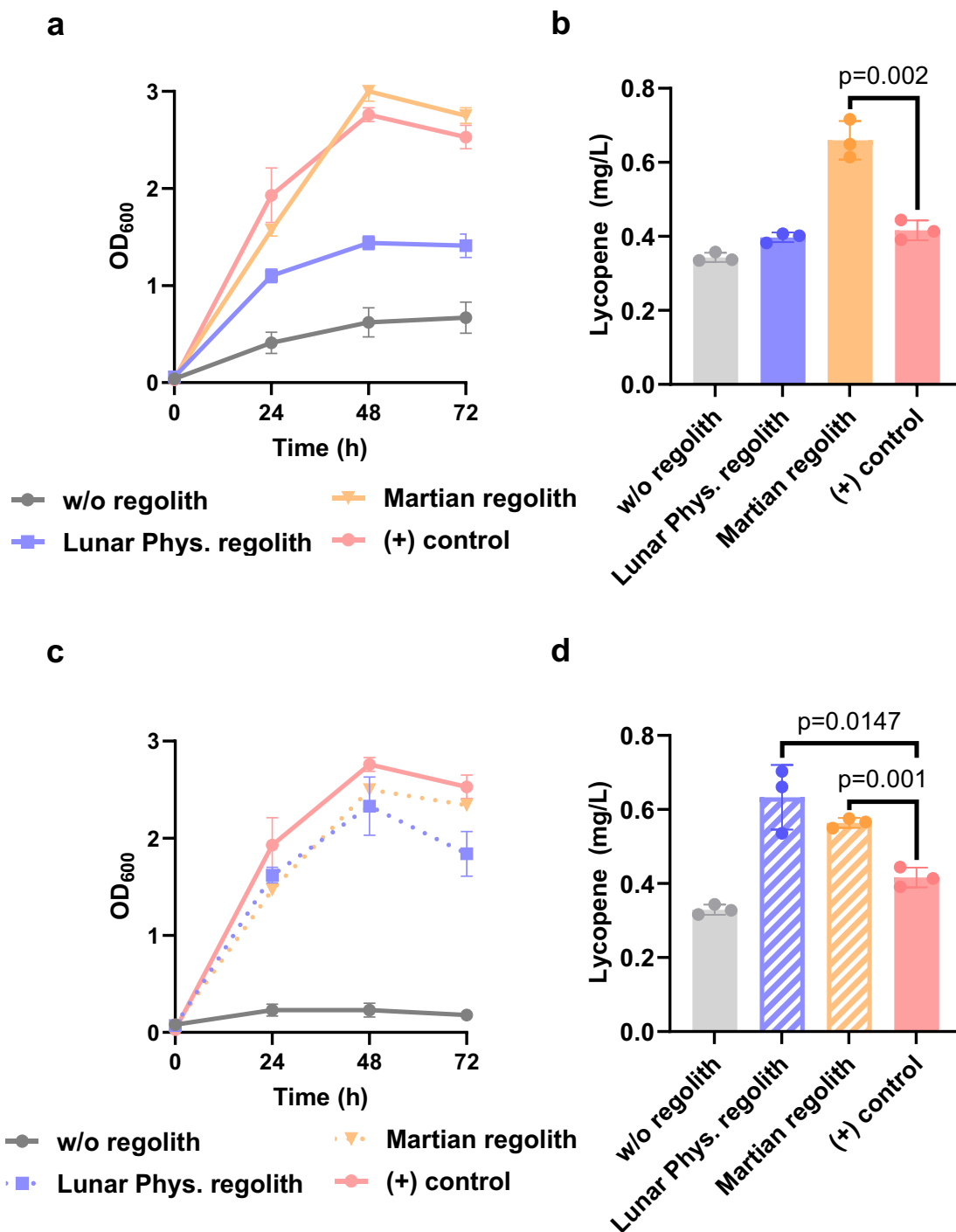


Fig. 4 | Producing lycopene in the semi-alternative medium. **a** Cell growth of RPET Strain S6 when cultivated in the semi-alternative medium with either Lunar or Martian regolith simulant particles as a mineral source. At each time point, a 200 μ L sample of the culture was taken to measure the cell density (OD_{600}). **b** Lycopene production assay for the RPET Strain S6 cultivated in different media, as indicated in (a). Cells were harvested at the end of the fermentation and then lyophilized before being subjected to lycopene assay. **c** Cell growth of RPET Strain S6 when cultivated in the semi-alternative medium with either acidified Lunar or Martian regolith simulant as a mineral source. At each time point, a 200 μ L sample of the culture was taken to measure the cell density (OD_{600}). **d** Lycopene production assay for the RPET S6 cultivated in different media, as indicated in (c). Cells were

harvested at the end of the fermentation and then lyophilized before being subjected to lycopene assay. RPET S6 cultivated in a regular minimal medium represents the positive control ((+) control). w/o regolith represents the RPET S6 cultivated in the minimal medium without minerals. In all the conditions, mimicked PET hydrolysate was supplied as a carbon source. The variations in the changes of the lycopene production were analyzed using an unpaired two-tailed *t*-test. The 95% confidence interval for the difference between means of particle and acidified Martian regolith simulant containing medium and positive control are -0.34 to -0.15 and -0.2 to -0.1 , respectively. All values represent the mean of triplicate cultures ($N=3$), with error bars depicting the standard deviation from that mean. Source data are provided as a Source Data file.

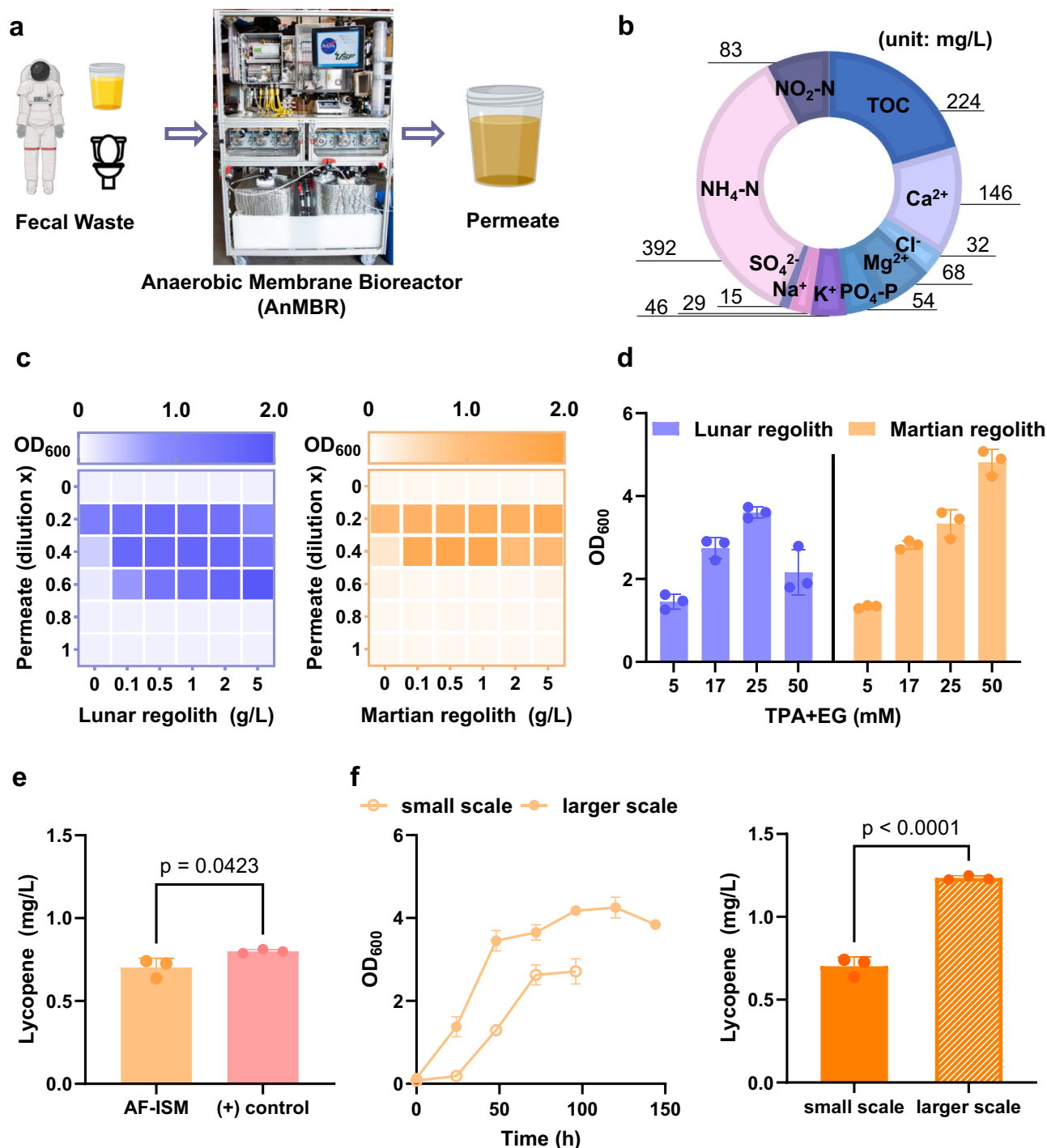


Fig. 5 | Developing a completely alternative medium for producing lycopene.

a Schematic diagram of fecal waste treatment using AnMBR. The resulting solution (permeate) was supposed to contain N and P sources. **b** Compositional analysis of AnMBR permeate using ion chromatography. **c** Extensive factorial experiment to optimize the concentrations of both regolith and permeate in the AF medium. RPET S6 was inoculated into the minimal medium with an identical concentration of carbon source but varying regolith and permeate concentrations. **d** Testing the RPET cell growth in the AF medium with varying carbon concentrations. RPET S6 was cultivated in the appropriate minimal media supplemented with TPA and EG at concentrations ranging from 5 mM to 50 mM each. **e** Comparison of lycopene production by RPET S6 in the AF medium versus a regular minimal medium. RPET S6 cultivated in the regular minimal medium represents the positive control ((+) control). The assay utilized 50 mM each of TPA and EG as the carbon source. The variations in lycopene production changes were analyzed using an unpaired two-

tailed *t*-test. The 95% confidence interval for the difference between means of Martian regolith simulant-based medium and positive control is 0.01 to 0.17.

f Scalability test of RPET S6 in the Martian regolith simulant-based AF medium supplemented with 40% permeate and 50 mM each of TPA and EG. Both cell growth (left panel) and lycopene production (right panel) were measured for comparison. Scaling up was conducted in a large flask (2-liter), and a small-scale fermentation was used as a control. At each time point, a 200 μ L sample of the culture was taken to measure the cell density (OD_{600}). After fermentation, 5 mL of cells were harvested for lycopene assay. The variations in lycopene production changes were analyzed using an unpaired two-tailed *t*-test. The 95% confidence interval for the difference between means of small- and large-scale is 0.45 to 0.62. All values represent the mean of triplicate cultures ($N=3$), with error bars depicting the standard deviation from that mean. Source data are provided as a Source Data file. Figure 5a was created with Biorender.com.

each could achieve individually, creating a more favorable environment for cell proliferation⁵⁹. Therefore, in our study, an extensive factorial experiment was conducted to evaluate the performance of the AF media prepared with different concentration combinations of regolith and permeate, with the goal of optimizing the formulation of the complete AF medium. Interestingly, our results showed that the addition of either Lunar or Martian regolith could restore the cell growth of RPET S6 in the medium, even at a permeate dilution factor greater than 0.2 (Fig. 5c). Additionally, when both regolith simulant concentrations were below 1.0 g/L (regardless of variations within this range), increasing the permeate dilution factor above 0.4 resulted in decreased final cell density (Fig. 5c). Furthermore, for the Martian regolith simulant, concentrations above 1.0 g/L were toxic to RPET cell growth under the 0.4-fold permeate condition (Fig. 5c). Intriguingly, however, a similar phenomenon was not observed at higher concentrations of the Lunar regolith simulant with permeate dilution factor set at 0.6 (Fig. 5c). Altogether, these results suggest a synergistic effect between regolith and permeate in supporting RPET growth, highlighting the importance of extensive factorial experiments in optimizing the formulation of the alternative feedstock medium to support microbial metabolism for sustainable biomanufacturing applications.

In addition to the supporting effects of the nutrients derived from permeate and regolith, carbon concentrations in the AF medium also play a critical role in determining the cell biomass accumulation and, ultimately, lycopene production. Despite the variability of Lunar regolith in supporting RPET cell growth, both regolith simulants were used at 1.0 g/L, and the permeate dilution factor was set at 0.4 for the subsequent carbon effect analysis. Our results showed that increasing the concentrations of TPA and EG (from 5 mM each to 50 mM each) led to a relatively higher final cell density (Fig. 5d). Nevertheless, under the Lunar regolith condition, RPET S6 cell growth significantly declined when the carbon concentration increased to 50 mM each (Fig. 5d), opening an interesting research avenue to explore the underlying mechanism of the carbon toxicity to RPET S6 in this type of AF medium.

Subsequently, we applied Human Exploration of Mars Design Reference Architecture 5.0 (DRA 5.0)⁶⁰ as the reference mission architecture to assess the feasibility of using AF medium for lycopene production. Specifically, RPET S6 was cultivated in either regular minimal medium or the corresponding AF medium (containing 1.0 g/L Martian regolith simulant and 0.4-fold diluted permeate) supplied with identical mimicked PET hydrolysate (50 mM each TPA and EG) as the carbon source. The subsequent assay revealed that lycopene production by RPET S6 in the AF medium was comparable to that in the positive control medium (Fig. 5e). Furthermore, we scaled up the fermentation to a large flask (2-liter) to assess the scalability of the process we developed. Our results showed that in the large-volume fermentation, RPET S6 rapidly entered the exponential phase, with significantly higher final cell density (OD₆₀₀) and lycopene production, compared to those obtained from small-scale tests (Fig. 5f). Moreover, the production level of lycopene was comparable with those reported in the literature when using alternative feedstocks as the carbon source (Supplementary Table 4). Overall, these findings demonstrated that the complete AF medium can effectively facilitate sustainable lycopene bioproduction by RPET S6 within the mission architecture of DRA 5.0.

Establishing alternative feedstock-driven in-situ biomanufacturing (AF-ISM) for in-space lycopene production

Compared to the Earth, space has unique environmental characteristics, including zero oxygen, microgravity, temperature fluctuations, and high radiation levels⁶¹. Undoubtedly, exposure to these stresses can severely disrupt the intracellular metabolism of living organisms, ultimately affecting the reproducibility of in-space biomanufacturing

in the complex space environment. Although microbial fermentation can be conducted in a sealed, well-controlled bioreactor to protect the microbial organisms from shortage of oxygen, temperature fluctuations, and high radiation levels⁶², the challenge of gravity difference remains difficult to overcome in off-world conditions. Moreover, it has been reported that gravity difference is one of the most significant factors affecting microbial cell growth and metabolism⁶³.

To demonstrate the proof-of-concept for in-space biomanufacturing, we developed a process termed alternative feedstock-driven in-situ biomanufacturing (AF-ISM) that validates the feasibility of lycopene production by RPET S6 using the AF medium under simulated microgravity conditions. Specifically, we first created the low shear modeled microgravity (LSMMG) using the High Aspect Ratio Vessels (HARVs) to simulate the microgravity condition (Fig. 6a). Then, RPET S6 was inoculated in the complete AF medium and cultivated in the simulated in-space condition for six days. Meanwhile, this strain cultivated in the Earth's gravity condition with the identical growth medium and vessel was used as a positive control. Our morphological comparison showed that cells cultivated in the simulated microgravity condition aggregated together, which is dramatically different from the cells cultivated in the Earth condition (Fig. 6b). More intriguingly, despite the incomplete consumption of the carbon source, cells cultivated in the simulated microgravity condition gave nearly identical lycopene production compared to that of the strain cultivated in the Earth condition (Fig. 6c, d). Taken together, our results revealed that AF-ISM could be a promising technology to facilitate the development of a long-term, self-sufficient life support system for space exploration.

Economic assessment of AF-ISM-based lycopene production within the mission architecture of DRA 5.0

The urgent need for developing ISRU to produce food, medicine, and oxygen to sustain humans on a long-term mission imposes critical ECLSS (Environmental Control and Life Support System) feasibility constraints⁶⁴. Notably, one of the key objectives of DRA 5.0 emphasizes that the Mars Human Habitability ISRU should address human health, environmental characterization, environmental hazard mitigation, and Mars resource utilization⁶⁰. In this study, we successfully produced lycopene from PET waste and in-situ resources (e.g., Martian regolith) using RPET S6, aligned directly with the objective of DRA 5.0. It has been reported that techno-economic analysis (TEA) is a valuable tool for estimating the economic performance of biomanufacturing processes and plays a crucial role in developing economically viable biochemical production technologies⁶⁵. To demonstrate the economic feasibility of the AF-ISM-based lycopene production process is superior to that of the conventional biomanufacturing process in supporting crewed missions on Mars, we used Equivalent Systems Mass (ESM) to quantitatively compare the specific attributes of AF-ISM with those of the conventional process reliant on regular logistical supplies from Earth (Fig. 7a). This is because ESM is an efficient method for evaluating the overall mass impact of a system by converting non-mass parameters, such as volume, power consumption, or crew time, into an equivalent mass value, providing a single, comparable metric for assessing different systems employed in space exploration²⁴.

In this study, to simplify the calculation, we assume a one-time trip to Mars for a long-term surface operation mission with four healthy crew members (-180 days out to Mars and -500 days on its surface). We further assume that the habitat assemblies and in-situ resource utilization hardware for biomanufacturing have been launched from Earth and assembled at the mission site. Foundational data—including the required values of the system and equivalency factors (Supplementary Table 5)—were obtained from the literature for ESM analysis^{24,25}. In the conventional medium scenario, all chemical components for lycopene bioproduction, except water, are supplied from Earth, whereas in the AF medium scenario, all feedstocks are sourced from the space environment. Our detailed analysis revealed that using

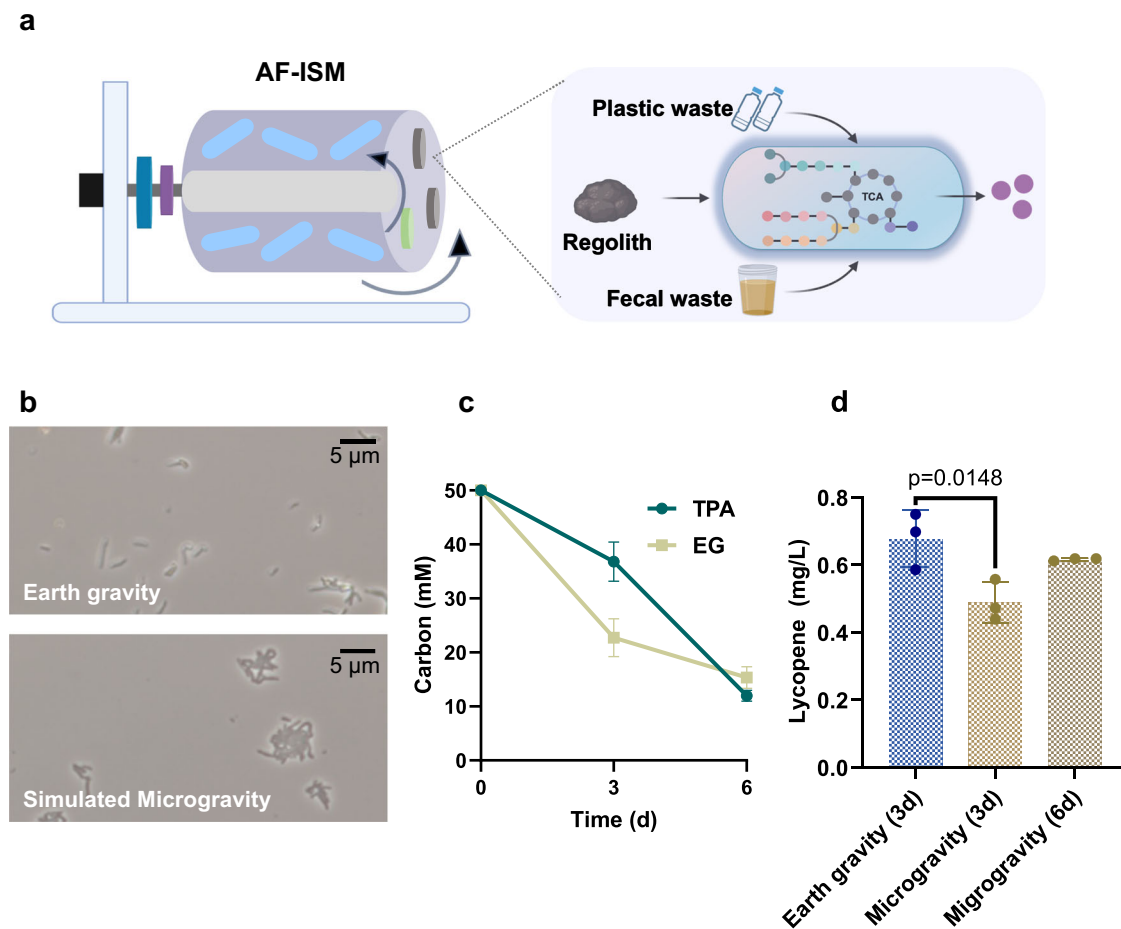


Fig. 6 | Validating AF-ISM for in-space biomanufacturing. **a** Schematic diagram of AF-ISM. The low shear modeled microgravity was created using the High Aspect Ratio Vessels (HARVs) system. RPET Strain S6 was inoculated into the completely alternative medium and cultivated in the simulated microgravity condition for evaluating AF-ISM in in-space biomanufacturing. **b** Morphological analysis of the RPET Strain S6 cultivated in either Earth or simulated microgravity conditions. Images are representative of $N=2$ independent experiments. **c** Consumption of TPA and EG by RPET Strain S6 when cultivated in a completely alternative medium under microgravity conditions. At each time point, a 200 μL sample of the culture

was taken to measure substrate concentrations. The cell suspension was centrifuged, and concentrations of TPA and EG were determined by HPLC. **d** Comparison of the lycopene production by RPET S6 when cultivated under either Earth or microgravity conditions. The variations in the changes in lycopene production were analyzed using an unpaired two-tailed t -test. The 95% confidence interval for the difference between means of Earth gravity (3 days) and microgravity (6 days) is -0.09 to 0.01 . All values represent the mean of triplicate cultures ($N=3$), with error bars depicting the standard deviation from that mean. Source data are provided as a Source Data file. Figure 6a was created with Biorender.com.

the AF medium for lycopene biomanufacturing resulted in a significantly lower ESM (Fig. 7b). Take together, these findings suggest that the AF-ISM process holds great potential as a practical platform for improving the sustainability and economy of Mars exploration. Moreover, with advancements in synthetic biology, we can envision that by exploiting the metabolic versatility of the microbial chassis deployed in in-space biomanufacturing, the economic feasibility of supplying food, energy, and materials for long-duration Mars exploration could be further enhanced through AF-ISM.

Discussion

Long-duration space exploration and potential settlements on other planets require innovative technologies to enable independence from terrestrial resources. In this study, we developed AF-ISM for sustainably producing consumable goods by effectively utilizing in-situ resources (i.e., regolith) and reclaiming resources from waste streams (i.e., waste plastic and fecal waste), emerging as a potentially pivotal technology for building long-term, self-sufficient life support systems for space exploration. In this bioprocess, all the nutrients essential for microbial biomanufacturing can be sourced from the in-situ resources and waste streams, thereby eliminating the dependence

on the resupply missions from Earth. In addition, we experimentally validated AF-ISM by producing lycopene—a food supplement—in a completely alternative medium under the simulated microgravity condition, demonstrating a strong economic feasibility. Overall, this proof-of-concept highlights AF-ISM as a promising approach for enabling long-duration and deep space exploration.

Even though metal elements are necessary nutrients for living organisms, some are also toxic and growth-limiting reagents, particularly the heavy metal ions^{47,66}. Therefore, understanding the qualitative and quantitative compositions of the regolith plays a pivotal role in developing it into an alternative feedstock for microbial biomanufacturing. One interesting finding from our study is that although the elemental contents of the Lunar chemical and physical regolith simulants are nearly identical, their effectiveness in supporting RPET S6 cell growth is dramatically different (Fig. 2a). Additionally, it has been reported that calcium homeostasis is crucial for bacterial cell stability⁶⁷. Bacteria have evolved a precise regulatory mechanism to efflux intracellular calcium and maintain homeostasis efficiently. When excessive free calcium ions accumulate near the cells, this balance would be disrupted, leading to irreversible cellular toxicity^{67,68}. Therefore, we hypothesized that the low tolerance of RPET S6 to the

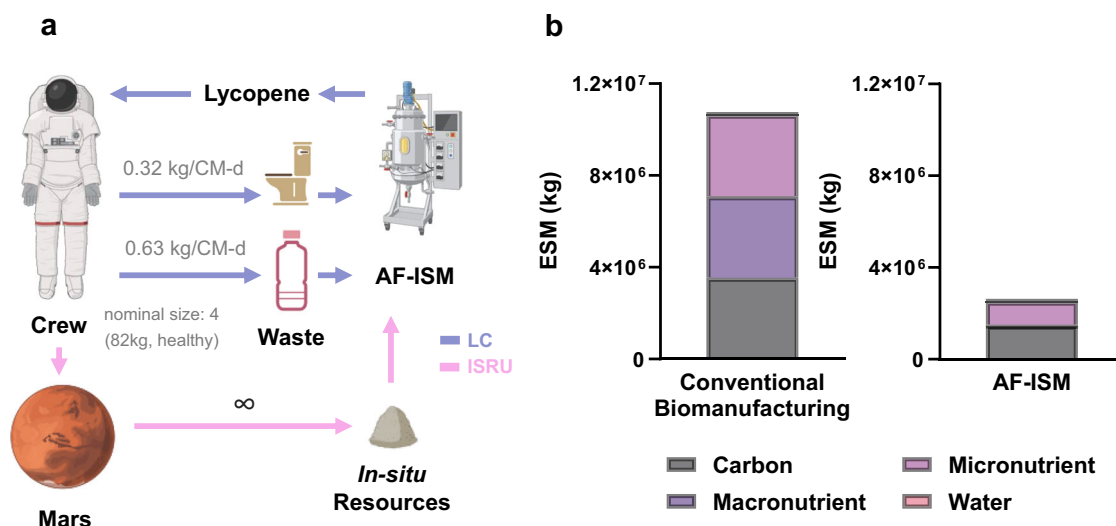


Fig. 7 | AF-ISM economic assessment within the mission architecture of DRA 5.0. **a** Concepts-of-operation for lycopene production through AF-ISM. Operations are illustrated using color-coded models: Loop-closure (LC, purple) and in-situ resource utilization (ISRU, pink). **b** Economic assessment of lycopene production using the conventional medium versus the AF medium. The required

values of the system and equivalency factors for ESM calculation are provided in Supplementary Table 5. Details of the ESM calculation can be found in the Method section. An example calculation can be found in Supplementary Method 1. Source data are provided as a Source Data file. Figure 7a was created with Biorender.com.

Lunar physical simulant might be due to calcium toxicity, as its concentration in the Lunar physical simulant is approximately 2-fold higher than that in the Lunar chemical simulant (Supplementary Table 1). Our subsequent metal toxicity test for Ca, Mg, Fe, Al, Cr, and Ti revealed no significant inhibition of RPET S6 cell growth with the addition of extra metal ions, except for calcium (Supplementary Fig. 3), validating our hypothesis to some extent. Overall, our results thereby underscore the necessity of testing the regolith sourced from different locations on the surfaces of the Moon and Mars, as the composition of either Lunar or Martian soil varies between these locations²⁰.

In this study, we demonstrate the feasibility of directly using regolith particles as a mineral replacement for microbial biomanufacturing, which holds great promise for making in-space biomanufacturing more economically viable. Although detailed control experiments determined that minerals could be leached from the regolith particles by their physical interactions with medium (Supplementary Table 3), our preliminary test of the regolith simulant utilization by model industrial hosts, including *Escherichia coli* and *Saccharomyces cerevisiae*, showed that neither species could experience growth support by the regolith simulant (Supplementary Fig. 4). These results suggested that the RPET strain possesses a unique ability to extract minerals from regolith particles. Unlike other species, it has been reported that the key mechanism for mineral degradation by RPET S6 is acidolysis⁶⁹. *Rhodococcus* species are known to secrete organic acids derived from the TCA cycle, particularly when using aromatics as the carbon source⁷⁰. Additionally, through their phosphate-solubilizing activity, other types of organic acids, such as gluconic acid, could be excreted by *Rhodococcus* species⁷¹. These metabolic features suggest that RPET S6 may be able to degrade the regolith simulant particles by secreting organic acids. Moreover, because of RPET S6's ability to biosynthesize and secrete chelating molecules, such as siderophores⁷², we thereby hypothesized that this could also promote the dissolution of regolith simulant particles by forming inner-sphere complexes at the mineral surface^{51,73}. In addition to acidolysis reactions, previous studies have reported that microorganisms can form biofilms at the fluid-mineral interface, creating a favorable microenvironment that protects themselves against environmental fluctuations⁷⁴. This characteristic also impacts the biological weathering process of the mineral⁵¹. Our FT-IR analysis confirmed that

RPET S6 could secrete extracellular polymeric substances (i.e., proteins) (Fig. 3c), which can assist the RPET S6 cells to attach to the surface of the regolith simulant particles. SEM imaging analysis (Fig. 3d) also confirmed this interaction between bacteria and regolith simulant particles. Furthermore, the rough and angular characteristics of the regolith simulant particle surface could facilitate the attachment of RPET S6 cells during growth. Taken together, our results demonstrate that leaching elements from regolith simulant particles to support RPET S6 cell growth is mediated through a combinatorial biochemical process.

The lycopene production assay for RPET S6, when cultivated in the minimal medium supplied with the regolith simulant or its particles, showed significant improvement compared to the positive control (Fig. 4). This suggests that replacing trace elements with regolith simulant-derived minerals in the growth medium may benefit lycopene biosynthesis in RPET S6. In our study, we found that the total concentration of metal ions was 12 to 17 mg/L when using the acidified regolith simulant as the trace element replacement, which is approximately 19.7- to 28.3-fold higher than that of the regular minimal medium (-0.58 mg/L of total metal ions). Previous studies have shown that oxidative stress caused by the addition of excess metal ions can enhance the production of antioxidant compounds, such as carotenoids⁷⁵. Therefore, we hypothesized that the oxidative stress caused by the high concentration of metals in the AF medium is likely a major factor in enhancing lycopene production in RPET S6. Additionally, we have identified that in RPET S6, the Methylerythritol 4-phosphate (MEP) pathway is responsible for supplying the two precursors, isopentenyl diphosphate (IPP) and dimethylallyl diphosphate (DMAPP), for terpenoid biosynthesis²⁶. Within this pathway, 1-Deoxy-d-xylulose-5-phosphate reductoisomerase (DXR) is a key enzyme that utilizes NADPH and divalent cation, either Mg²⁺ or Mn²⁺, as cofactors^{76,77}. Studies have also shown that binding with Mn²⁺ results in higher enzymatic activity and stability of DXR⁷⁸, potentially redirecting more carbon flux toward the carotenoid biosynthetic pathway. Intriguingly, RPET S6 produced nearly identical levels of lycopene when cultivated in the regular minimal medium regardless of the presence or increase in Mn²⁺ concentrations (Supplementary Fig. 5). These results indicate that the native MEP pathway in RPET S6 has a low dependency on specific divalent cations to maintain its activity, suggesting that

RPET S6 could serve as a promising and robust chassis for in-space biomanufacturing applications. Moreover, the underlying molecular mechanisms by which the specific metal ions, as well as the oxidative stress, influence the carbon flux toward the carotenoid biosynthetic pathway in RPET S6 still need to be thoroughly investigated.

The successful evaluation of the regolith simulant performance led to the development of a completely alternative medium by replacing macronutrient sources with the AnMBR permeate (Fig. 5). Testing tolerance of RPET S6 cells to the permeate helped determine its optimal dosage for cell growth in the absence of regolith (Supplementary Fig. 2). This effort also revealed toxicity associated with the complex matrix of the fecal waste, particularly at high dilution factors. Notably, the compositional analysis of the permeate revealed a significant amount of nitrite (ammonium:nitrite = 4.7:1) accumulated (likely due to partial nitrification), which may be the primary factor contributing to cell growth inhibition in RPET S6. Interestingly, the addition of the regolith simulant enhanced RPET S6's tolerance to permeate toxicity (Fig. 5c). One possible explanation for this observed synergistic effect is the high content of Mn in the regolith, as Mn has been identified as a key element in mitigating nitrite inhibition by catalyzing nitrite oxidation into (nontoxic) nitrate under physiological conditions and by influencing processes involving reactive oxygen species (ROS)⁷⁹. In addition, the long-term stability test of the RPET S6 strain in the AF medium showed that the final cell density of the strain remained unchanged even after 28 days of subculture, while the final lycopene production was decreased slightly (Supplementary Fig. 6). Since no significant cell growth difference was observed, we hypothesized that the slight reduction in lycopene production may be due to the loss of the lycopene producing plasmid, likely resulting from the inherent metabolic burden of maintaining self-replicating plasmids in the RPET strain^{26,33}.

Beyond Earth, the utilization of the developed medium has the potential of an actual application for the space mission, first confirmed by the microgravity simulation test. RPET S6 is robust in the diminished gravity, repurposing their aggregating ability to survive by adapting to environmental changes such as the antimicrobial environment^{80,81}. The quasi-stationary movement under microgravity does not hinder the final lycopene production, even though the production was delayed compared to the Earth's gravity condition. Additionally, previous studies have demonstrated that oxygen can be produced through the electrolysis of water or regolith in molten salts or oxides⁸². In another study, under energy conditions similar to those of the Mars Oxygen In-Situ Resource Utilization Experiment (MOXIE), Kelly et al. explored the potential of microwave (MW)-plasma-based in-situ utilization of the Martian atmosphere, achieving an oxygen production rate of 47.0 g/L⁸³. These proof-of-concept studies have established the potential for achieving an efficient on-site supply of oxygen using in-situ resources, laying the foundation for applying obligate aerobic microbial chassis (e.g., RPET S6) in off-world biomanufacturing. Regarding the water supply in the extra-terrestrial condition, producing water from lunar ilmenite through reaction with endogenous hydrogen has been validated⁸⁴. This approach could help address the water supply concern for off-world biomanufacturing. Taken together, the advancements of technologies for efficiently producing the basic components required for fermentation on-site eliminate reliance on Earth's resupply and competition for its resources, ultimately enabling cost-effective off-world biomanufacturing.

In conclusion, we propose AF-ISM employing versatile RPET S6 to utilize alternative feedstocks for efficient biomanufacturing of lycopene. Economically friendly technologies that can significantly reduce the need for raw materials from Earth resupply will play a critical role in space exploration. Compared to the conventional method, the alternative feedstock-derived biomanufacturing process demonstrates lower dependency on logistic support from Earth, resulting in

dramatically reduced production costs (Fig. 7). Although promising, further verification of our technologies in diverse space conditions such as experiments in ISS will be essential to confirm their reliability before deploying the microbial factory on space missions. Nevertheless, our core technologies will also be useful for addressing global issues of plastic waste, human waste, pollution, biomineralization of rare earth elements, and sustainable production of chemicals and materials^{85,86}.

Methods

Bacterial strain and cell growth test

The RPET variant strain S6 (RPET S6) was developed for upcycling PET to lycopene²⁶. The seed culture of the strain was prepared in the Greasham medium (control medium; Supplementary Table 6) supplied with 5 g/L glucose as the carbon source and 20 µg/ml gentamycin. Unless otherwise noted, all the cultures were incubated at 30 °C with shaking at 250 rpm in the dark condition.

For the nutrient dosage test, RPET S6 was cultivated in the glass test tube with a working volume of 10 ml. The culture condition for each experiment was specified in the corresponding figure legend. RPET S6 was inoculated into a 125-ml flask with a working volume of 25 ml for lycopene production assay in the semi-alternative medium. The positive control for all tests is a culture in the Greasham medium containing 17 mM each of TPA and EG. For the factorial experiment, RPET S6 was inoculated into the corresponding media (equimolar mixtures of TPA and EG as the carbon source) for cell growth tests, with varying dilutions of permeate (0, 0.2, 0.4, 0.6, 0.8, 1.0-fold) and multiple concentrations of regolith simulants (0, 0.2, 0.5, 1.0, 2.0, and 5.0 g/L). To assess the effects of carbon concentration on cell growth, RPET S6 was inoculated into a minimal medium supplemented with 1 g/L regolith, 40% permeate, and varying concentrations of TPA and EG, ranging from 5 mM each to 50 mM each. 20 µg/ml gentamycin was provided for every culture to maintain the lycopene-producing plasmid. The optical density at 600 nm (OD₆₀₀) was measured in VWR semimicro polystyrene cuvettes, using a Tecan Infinite M200 Pro plate reader (Tecan, Switzerland). Abs₆₀₀ (absorbance) values were converted into OD₆₀₀ values by the experimentally determined relationship, OD₆₀₀ = 1.75 × Abs₆₀₀.

Alternative feedstocks preparation

The selection criteria of the regolith simulant were based on the representation capability of the actual regolith by the high-fidelity. Lunar regolith simulants of Black Point One (BP-1) and Johnson Space Center One (JSC-1/1A) were provided by NASA, showing physical similarity of rough and angular particle shape⁸⁷ and chemical similarity to the soil from the geological terrain of the Moon, respectively. The Martian regolith simulant of Martian Global (MGS-1) was purchased from Space Resource Technologies, FL, USA. MGS-1 is a mineralogical standard for basaltic soils on Mars, developed based on quantitative mineralogy from the Mars Science Laboratory Curiosity rover. For the particle simulant utilization test, 100 g/L of stock solution was prepared in the sterilized water. For the acidified simulant utilization test, 100 g/L of stock solution was prepared in the 1% nitric acid solution. The metal leaching in the acidic (pH = 1) solution lasted for 24 h. The solution was filtered out using a 0.22 µm polyethersulfone membrane.

The dissolution of titanium, aluminum, magnesium, iron, manganese, and chromium was quantified using the Inductively Coupled Plasma Mass Spectrometry (ICP-MS) using NexION 2000 (PerkinElmer, Waltham, MA). The pressure of argon gas was 100 psi, and the sample flushing time was 45 s for the 3 ml samples. The calibration curve was prepared by the serial dilution of the standard from 0 to 100 µg/L. Calcium, sodium, and potassium dissolution were analyzed using cation chromatography using IonPac CS12A of Dionex Easion (Thermo Scientific, USA). Samples were diluted in the deionized water. The range of the standard curve was 0–50 mg/L.

TPA and EG stock were prepared by dissolving them in deionized water overnight in dark conditions. For the AnMBR permeate preparation, the canine fecal waste was treated using the Organic Processor Assembly (OPA) unit. The treatment capacity of the influent is 2.5 L per day to mimic that of a crew of four astronauts. The treated fecal material is ultrafiltered through a specialized membrane module and collected at a rate of 2.5 L/day. All feedstocks were filter sterilized before the cultivation.

Post-consumer PET alkaline hydrolysis was carried out using a method derived from our previous study with modifications²⁶. Briefly, post-consumer PET bottles were collected and cut into 0.5 × 0.5 cm pieces. Then, 6 g of PET chunks were added to a 60 mL aqueous solution (2 M NaOH). The homogeneous suspension was then fed into the PTFE vessel. The PET decomposition reaction was conducted in a Parr Stirred Reactor (Series 4560 Mini Reactors, 100–600 mL) at 180 °C for 2 h with agitation. The reaction mixture was cooled on ice and centrifuged at 3500 × g for 10 min to remove unreacted PET solids. The clear supernatant was then neutralized to pH 7.0 with HCl. The concentrations of the resulting monomers were determined prior to being transferred to the microbial cultures.

Particle simulant utilization analysis

Cultivated samples were vacuum filtered through Grade 2 Qualitative Filter Paper (pore size: 8 μm; Whatman, Maidstone, UK) and washed three times using deionized water violently. The filter paper with simulant particles was air-dried completely before all analysis. The iS20 FT-IR Spectrometer (Nicolet, Prague, CZ) was used to determine the surface functional group change of particle simulants before and after the RPET S6 growth. The sample covered the sample loading area entirely for data quality assurance. The measurement conditions were a wavenumber range of 400–4000 cm⁻¹, 2–4 resolution, and 32 scans. The data was acquired as the transmittance (%), and OMNIC was the data collection software. The background was collected before every sample.

Quattro S Environmental SEM (Thermo Scientific, USA) was used to characterize the surface morphology and adsorption. Double-sided carbon tape was attached to the metal holder for the sample preparation. Then, a thin layer of sample was mounted on the carbon tape. The working distance was 10 mm. For the distribution of mineral components, an X-ray diffraction analysis was performed using Bruker d8 Advance X-ray Diffractometer. The instrument was operated at 40 kV and 40 mA. The sample was mounted in the MTI low background Si disc Zero Diffraction Plate. XRD patterns were collected in the 2θ range of 15–80° with a step size of 0.5°. The samples were analyzed under ambient conditions. The scanned XRD patterns were processed using Bruker Diffrac.Eva.

Substrate and lycopene quantification

TPA concentration was measured using Agilent 1260 Infinity II high-performance liquid chromatography (HPLC) system (Agilent Technologies, USA) equipped with the Agilent Poroshell 120 EC-C18 column (4.6 × 100 mm, 2.7 μm) and a diode array detection (DAD), as described by our recent study²⁶. The column temperature was maintained at 60 °C, the DAD was set to 280 nm, and the flow rate was 1.0 mL/min. The mobile phase composition—consisting of phase A (water with 0.1% formic acid) and phase B (acetonitrile with 0.1% formic acid)—was adjusted over time using gradient elution as follows: 92:8 (A:B) at 0 min, 74:26 at 5 min, 50:50 at 8 min, and returned to 92:8 at 10 min. TPA concentration in the sample was determined by comparing UV absorbance values to a standard TPA calibration curve with an R² coefficient of ≥ 0.995.

EG quantification was performed using an Agilent 1260 Infinity II HPLC system equipped with an Aminex HPX-87H ion exclusion column (300 mm × 3.78 mm, 9 μm particle size; Bio-Rad, USA) and a refractive index detector (RID), as described by our recent study²⁶.

The column temperature was maintained at 40 °C, and samples were isocratically eluted with 0.01N H₂SO₄ as the mobile phase at a flow rate of 1.0 mL/min. EG concentration in the sample was determined by comparing peak area values to a standard EG calibration curve with an R² coefficient of ≥ 0.995.

Lycopene extraction and HPLC assay were performed using a method described in our previous study²⁶. For lycopene extraction, 5 mL aliquots of cells were centrifuged at 3500 × g for 10 min, washed with deionized water, and then lyophilized. The dry cell pellets were resuspended in a methanol/acetone solution (500 μL; 7:3, v/v) containing 0.05% butylated hydroxytoluene (BHT) and disrupted using ZR BashingBead Lysis Tubes (0.1 mm beads; Zymo Research, USA) in a BeadBug™ microtube homogenizer (Benchmark Scientific, USA) at 4000 rpm for 3 min. After centrifugation, the supernatant was transferred to a 1.5 mL tube. This process was repeated until the supernatant showed no visible color. The organic phase containing lycopene was filtered through a 0.22 μm syringe filter into an amber glass vial for HPLC analysis. Quantification of lycopene was performed using Agilent 1260 Infinity II HPLC system equipped with an EC-C18 column and a DAD detector set at 474 nm. The column temperature was maintained at 40 °C, and samples were isocratically eluted over 15 min at a constant flow rate of 1.5 mL/min. The mobile phase consisted of a methanol/acetonitrile solution (7:3, v/v). Lycopene concentration in the sample was determined by comparing absorbance values to a standard lycopene calibration curve with an R² coefficient of ≥ 0.995.

Microgravity simulation

Simulated microgravity experiments were performed using High Aspect Ratio Vessels (HARVs) (Synthecon, Inc., Houston, TX), which are specialized ground-based bioreactors designed to create a low-shear modeled microgravity environment for the cells growing in them. The overnight grown primary culture was diluted to an initial OD₆₀₀ of 0.1 using a fresh culture medium, and 10 mL of culture volume was loaded into HARVs in a sterile manner. Residual air bubbles were removed through a syringe port. Cells were constantly aerated through a gas-permeable membrane present on one side of the vessel. Four different rotation speeds (RPM) were tested to optimize the growth of cells in HARVs. The final growth experiments in simulated microgravity were conducted at RPM 7.2 and by placing the HARVs inside a static incubator at 30 °C. Samples were harvested on day 3 and day 6 to measure growth and lycopene production. The changes in cellular morphology due to the microgravity environment were investigated using Zeiss Axioplan 2 Upright Light Microscope (Carl Zeiss, Oberkochen, DE), and imaging was done using ZEN Blue 2.3 Pro software.

Equivalent Systems Mass calculation

The Equivalent Systems Mass (ESM) calculation using an established equation (Eq. 1)²⁵ was based on relevant literature. Because the final AF-ISM aimed at Martian regolith utilization, we set all baselines of this economics study for the mission on Mars (L_{eq} : location factor, M : mass of the system, V : volume of the system, V_{eq} : volume equivalency factor, C : cooling requirement of the system, C_{eq} : cooling equivalency factor, P : power, P_{eq} : power equivalency factor, CT : crew time, D : mission duration, and CT_{eq} : crew time equivalency factor).

$$ESM = Leq \cdot \left\{ M + (V \cdot V_{eq}) + (P \cdot P_{eq}) + (C \cdot C_{eq}) + (CT \cdot D \cdot CT_{eq}) \right\} \quad (1)$$

To compare the conventional medium, which needs the supply from the ground, with the AF medium that this study developed, all required values of the system and equivalency factors were obtained from the literature (Supplementary Table 5)²⁴. The control scenario (Scenario 1) is shipping all chemical components from the ground except for the water. Carbon sources of 5 kg/m³, macronutrients of 5.22 kg/m³, and micronutrients of 0.005 kg/m³ are required for the

conventional medium. The test scenario (Scenario 2) gets all the components from the space environment. Plastic of 3.88 kg/m³, regolith of 1 kg/m³, and fecal waste-treated water of 400 kg/m³ are required for the AF medium. ESM was calculated based on the system characteristics and factors. An example calculation can be found in Supplementary Method 1.

Statistical & Reproducibility

All experimental biological replicates, along with the number of data points used in the analysis where applicable, are detailed in the corresponding figure legends. Statistical analysis was performed using GraphPad Prism version 10. Descriptive statistics on mean and standard error were presented. To determine the significant difference between the two independent groups, unpaired two-tailed *t*-test was conducted, and *t*-statistic and *p*-value were calculated by the software. The 95% confidence interval was applied.

Reporting summary

Further information on research design is available in the Nature Portfolio Reporting Summary linked to this article.

Data availability

Data supporting the findings of this work are available within the main article and its Supplementary Information file. Source data are provided with this paper.

References

- Creech, S., Guidi, J. & Elburn, D. in *2022 IEEE Aerospace Conference (Aero)*. 1–7 (IEEE).
- Guerrero-Gonzalez, F. J. & Zabel, P. System analysis of an ISRU production plant: Extraction of metals and oxygen from lunar regolith. *Acta Astronautica* **203**, 187–201 (2023).
- Spohn, T., Breuer, D. & Johnson, T. *Encyclopedia of the solar system*. (Elsevier, 2014).
- Ferrone, K., Taylor, A. & Helvajian, H. In situ resource utilization of structural material from planetary regolith. *Adv. Space Res.* **69**, 2268–2282 (2022).
- Wang, Y. et al. In-situ utilization of regolith resource and future exploration of additive manufacturing for lunar/martian habitats: A review. *Appl. Clay Sci.* **229**, 106673 (2022).
- Cockell, C. S. Bridging the gap between microbial limits and extremes in space: space microbial biotechnology in the next 15 years. *Microb. Biotechnol.* **15**, 29–41 (2022).
- Nickerson, C. A., Medina-Colorado, A. A., Barrila, J., Poste, G. & Ott, C. M. A vision for spaceflight microbiology to enable human health and habitat sustainability. *Nat. Microbiol.* **7**, 471–474 (2022).
- Llorente, B., Williams, T. C., Goold, H. D., Pretorius, I. S. & Paulsen, I. T. Harnessing bioengineered microbes as a versatile platform for space nutrition. *Nat. Commun.* **13**, 6177 (2022).
- Benoit, M. et al. Microbial antibiotic production aboard the International Space Station. *Appl. Microbiol. Biotechnol.* **70**, 403–411 (2006).
- Lam, K. et al. The effect of space flight on the production of actinomycin D by *Streptomyces plicatus*. *J. Ind. Microbiol. Biotechnol.* **29**, 299–302 (2002).
- Moore, C. L. Technology development for human exploration of Mars. *Acta Astronautica* **67**, 1170–1175 (2010).
- Nangle, S. N. et al. The case for biotech on Mars. *Nat. Biotechnol.* **38**, 401–407 (2020).
- Keller, R. J. et al. Biologically-based and physiochemical life support and in situ resource utilization for exploration of the solar system—reviewing the current state and defining future development needs. *Life* **11**, 844 (2021).
- Montague, M. et al. The role of synthetic biology for in situ resource utilization (ISRU). *Astrobiology* **12**, 1135–1142 (2012).
- Castelein, S. M. et al. Iron can be microbially extracted from Lunar and Martian regolith simulants and 3D printed into tough structural materials. *PLoS ONE* **16**, e0249962 (2021).
- Berliner, A. J. et al. Space bioprocess engineering on the horizon. *Commun. Eng.* **1**, 13 (2022).
- Kruyer, N. S., Realff, M. J., Sun, W., Genzale, C. L. & Peralta-Yahya, P. Designing the bioproduction of Martian rocket propellant via a biotechnology-enabled in situ resource utilization strategy. *Nat. Commun.* **12**, 6166 (2021).
- Grier, J. & Rivkin, A. S. *Airless bodies of the inner solar system: Understanding the process affecting rocky, airless surfaces*. (Elsevier, 2018).
- De Micco, V. et al. Plant and microbial science and technology as cornerstones to Bioregenerative Life Support Systems in space. *npj Microgravity* **9**, 69 (2023).
- Lehner, B. et al. in Proc. 69th International Astronautical Congress, IAC-18, A1, 7, 7, x42645. 1–7.
- Santomartino, R. et al. Toward sustainable space exploration: a roadmap for harnessing the power of microorganisms. *Nat. Commun.* **14**, 1391 (2023).
- Lasseur, C. & Mergeay, M. Current and future ways to closed life support systems: virtual MELISSA conference, Ghent (B)(3-5/11/2020). A review. *Ecol. Eng. Environ. Prot.* **1**, 25–35 (2021).
- García Martínez, J. B., Alvarado, K. A., Christodoulou, X. & Denkenberger, D. C. Chemical synthesis of food from CO₂ for space missions and food resilience. *J. CO₂ Utilization* **53**, 101726 (2021).
- Averesch, N. J. H. et al. Microbial biomanufacturing for space-exploration—what to take and when to make. *Nat. Commun.* **14**, 2311 (2023).
- Ewert, M. K., Chen, T. T. & Powell, C. D. Life support baseline values and assumptions document. (2022).
- Diao, J., Hu, Y., Tian, Y., Carr, R. & Moon, T. S. Upcycling of poly(ethylene terephthalate) to produce high-value bio-products. *Cell Rep.* **42**, 111908 (2023).
- Sullivan, K. P. et al. Mixed plastics waste valorization through tandem chemical oxidation and biological funneling. *Science* **378**, 207–211 (2022).
- Tiso, T. et al. Towards bio-upcycling of polyethylene terephthalate. *Metab. Eng.* **66**, 167–178 (2021).
- Werner, A. Z. et al. Tandem chemical deconstruction and biological upcycling of poly(ethylene terephthalate) to β-ketoadipic acid by *Pseudomonas putida* KT2440. *Metab. Eng.* **67**, 250–261 (2021).
- Jehanno, C. et al. Critical advances and future opportunities in upcycling commodity polymers. *Nature* **603**, 803–814 (2022).
- Franden, M. A. et al. Engineering *Pseudomonas putida* KT2440 for efficient ethylene glycol utilization. *Metab. Eng.* **48**, 197–207 (2018).
- Santo, M., Weitsman, R. & Sivan, A. The role of the copper-binding enzyme – laccase – in the biodegradation of polyethylene by the actinomycete *Rhodococcus ruber*. *Int. Biodeterior. Biodegrad.* **84**, 204–210 (2013).
- Diao, J., Tian, Y., Hu, Y. & Moon, T. S. Producing multiple chemicals through biological upcycling of waste poly(ethylene terephthalate). *Trends in Biotechnology*, <https://doi.org/10.1016/j.tibtech.2024.10.018> (2024).
- Hu, Y., Tian, Y., Zou, C. & Moon, T. S. The current progress of tandem chemical and biological plastic upcycling. *Biotechnol. Adv.* **77**, 108462 (2024).
- Sibonga, J. D. et al. Recovery of spaceflight-induced bone loss: bone mineral density after long-duration missions as fitted with an exponential function. *Bone* **41**, 973–978 (2007).
- Matsumoto, A. et al. Weight loss in humans in space. *Aviat. space Environ. Med.* **82**, 615–621 (2011).
- Leach, C. S., Dietlein, L. F., Pool, S. L. & Nicogossian, A. E. Medical considerations for extending human presence in space. *Acta Astronautica* **21**, 659–666 (1990).

38. Bermudez-Aguirre, D., Cooper, M., Douglas, G. & Smith, S. in *Human Research Program Investigators' Workshop*.
39. Douglas, G. L., Zwart, S. R. & Smith, S. M. Space food for thought: challenges and considerations for food and nutrition on exploration missions. *J. Nutr.* **150**, 2242–2244 (2020).
40. Heinicke, C. & Arnhof, M. A review of existing analog habitats and lessons for future lunar and Martian habitats. *REACH* **21-22**, 100038 (2021).
41. Round, J. W., Robeck, L. D. & Eltis, L. D. An integrative toolbox for synthetic biology in *Rhodococcus*. *ACS Synth. Biol.* **10**, 2383–2395 (2021).
42. Warhurst, A. M. & Fewson, C. A. Biotransformations catalyzed by the genus *Rhodococcus*. *Crit. Rev. Biotechnol.* **14**, 29–73 (1994).
43. Anthony, W. E. et al. Development of *Rhodococcus opacus* as a chassis for lignin valorization and bioproduction of high-value compounds. *Biotechnol. Biofuels* **12**, 1–14 (2019).
44. Round, J. W., Roccor, R. & Eltis, L. D. A biocatalyst for sustainable wax ester production: re-wiring lipid accumulation in *Rhodococcus* to yield high-value oleochemicals. *Green. Chem.* **21**, 6468–6482 (2019).
45. Chatterjee, A., DeLorenzo, D. M., Carr, R. & Moon, T. S. Bioconversion of renewable feedstocks by *Rhodococcus opacus*. *Curr. Opin. Biotechnol.* **64**, 10–16 (2020).
46. Davis, K. & Moon, T. S. Tailoring microbes to upgrade lignin. *Curr. Opin. Chem. Biol.* **59**, 23–29 (2020).
47. Dong, H. et al. A critical review of mineral–microbe interaction and co-evolution: mechanisms and applications. *Natl Sci. Rev.* **9**, nwac128 (2022).
48. Ray, C., Reis, S., Sen, S. & O'Dell, J. JSC-1A lunar soil simulant: characterization, glass formation, and selected glass properties. *J. Non-Crystalline Solids* **356**, 2369–2374 (2010).
49. Cannon, K. M., Britt, D. T., Smith, T. M., Fritsche, R. F. & Batchelder, D. Mars global simulant MGS-1: A Rocknest-based open standard for basaltic martian regolith simulants. *Icarus* **317**, 470–478 (2019).
50. Lehner, B. A. et al. End-to-end mission design for microbial ISRU activities as preparation for a moon village. *Acta Astronautica* **162**, 216–226 (2019).
51. Wild, B., Gerrits, R. & Bonneville, S. The contribution of living organisms to rock weathering in the critical zone. *npj Mater. Degrad.* **6**, 98 (2022).
52. King, S., French, M., Bielefeld, J. & Lanford, W. Fourier transform infrared spectroscopy investigation of chemical bonding in low-k a-SiC: H thin films. *J. Non-Crystalline Solids* **357**, 2970–2983 (2011).
53. Gupta, J., Rathour, R., Dupont, C. L., Kaul, D. & Thakur, I. S. Genomic insights into waste valorized extracellular polymeric substances (EPS) produced by *Bacillus* sp. ISTL8. *Environ. Res.* **192**, 110277 (2021).
54. Liao, X. et al. Synergistic enhancement of metal extraction from spent Li-ion batteries by mixed culture bioleaching process mediated by ascorbic acid: Performance and mechanism. *J. Clean. Prod.* **380**, 134991 (2022).
55. Schneider, W. et al. NASA environmental control and life support technology development and maturation for exploration: 2019 to 2020 overview. *2020 International Conference on Environmental Systems* (2020).
56. Bullard, T. et al. A Prototype Early Planetary Organic Processor Assembly (OPA) Based on Dual-Stage Anaerobic Membrane Bioreactor (AnMBR) for Fecal and Food Waste Treatment and Resource Recovery. In *50th International Conference on Environmental Systems*, no. ICES-2021-323. 2021 (2021).
57. Anderson, M. S., Ewert, M. K. & Keener, J. F. Life support baseline values and assumptions document. (2018).
58. Wignarajah, K., Litwiller, E., Fisher, J. W. & Hogan, J. Simulated human feces for testing human waste processing technologies in space systems. *SAE Transactions*, 424–430 (2006).
59. Deng, Y.-J. & Wang, S. Y. Synergistic growth in bacteria depends on substrate complexity. *J. Microbiol.* **54**, 23–30 (2016).
60. Drake, B. G., Hoffman, S. J. & Beaty, D. W. in *2010 IEEE aerospace conference*. 1-24 (IEEE).
61. Thirsk, R., Kuipers, A., Mukai, C. & Williams, D. The space-flight environment: the International Space Station and beyond. *Cmaj* **180**, 1216–1220 (2009).
62. Walther, I. Space bioreactors and their applications. *Adv. Space Biol. Med.* **8**, 197–213 (2002).
63. Huang, B., Li, D.-G., Huang, Y. & Liu, C.-T. Effects of spaceflight and simulated microgravity on microbial growth and secondary metabolism. *Mil. Med. Res.* **5**, 1–14 (2018).
64. Berliner, A. J. et al. Towards a biomanufacturing on Mars. *Front. Astron. Space Sci.* **8**, 711550 (2021).
65. Fu, R., Kang, L., Zhang, C. & Fei, Q. Application and progress of techno-economic analysis and life cycle assessment in biomanufacturing of fuels and chemicals. *Green. Chem. Eng.* **4**, 189–198 (2023).
66. Wang, Z. et al. Anti-microbial activities of aerosolized transition metal oxide nanoparticles. *Chemosphere* **80**, 525–529 (2010).
67. King, M. M., Kayastha, B. B., Franklin, M. J. & Patrauchan, M. A. Calcium regulation of bacterial virulence. *Calcium Signal.* **1131**, 827–855 (2020).
68. Anderson, S., Appanna, V. D., Huang, J. & Viswanatha, T. A novel role for calcite in calcium homeostasis. *FEBS Lett.* **308**, 94–96 (1992).
69. Lambers, H., Nascimento, D. L., Oliveira, R. S. & Shi, J. Do cluster roots of red alder play a role in nutrient acquisition from bedrock? *Proc. Natl. Acad. Sci. USA* **116**, 11575–11576 (2019).
70. Roell, G. W. et al. A concerted systems biology analysis of phenol metabolism in *Rhodococcus opacus* PD630. *Metab. Eng.* **55**, 120–130 (2019).
71. Chen, Y. P. et al. Phosphate solubilizing bacteria from subtropical soil and their tricalcium phosphate solubilizing abilities. *Appl. Soil Ecol.* **34**, 33–41 (2006).
72. Bosello, M., Robbel, L., Linne, U., Xie, X. & Marahiel, M. A. Biosynthesis of the siderophore rhodochelin requires the coordinated expression of three independent gene clusters in *Rhodococcus jostii* RHA1. *J. Am. Chem. Soc.* **133**, 4587–4595 (2011).
73. Golubev, S. V. & Pokrovsky, O. S. Experimental study of the effect of organic ligands on diopside dissolution kinetics. *Chem. Geol.* **235**, 377–389 (2006).
74. Flemming, H.-C. & Wingender, J. The biofilm matrix. *Nat. Rev. Microbiol.* **8**, 623–633 (2010).
75. Cai, M., Li, Z. & Qi, A. Effects of iron electrovalence and species on growth and astaxanthin production of *Haematococcus pluvialis*. *Chin. J. Oceanol. Limnol.* **27**, 370–375 (2009).
76. Murkin, A. S., Manning, K. A. & Kholodar, S. A. Mechanism and inhibition of 1-deoxy-D-xylulose-5-phosphate reductoisomerase. *Bioorg. Chem.* **57**, 171–185 (2014).
77. Chen, A. Y. et al. Targeting metalloenzymes for therapeutic intervention. *Chem. Rev.* **119**, 1323–1455 (2018).
78. Cai, G. et al. Thermodynamic investigation of inhibitor binding to 1-deoxy-d-xylulose-5-phosphate reductoisomerase. *ACS Med. Chem. Lett.* **3**, 496–500 (2012).
79. Zerfaß, C., Christie-Oleza, J. A. & Soyer, O. S. Manganese oxide biomineralization provides protection against nitrite toxicity in a cell-density-dependent manner. *Appl. Environ. Microbiol.* **85**, e02129–02118 (2019).
80. Lynch, S., Mukundakrishnan, K., Benoit, M., Ayyaswamy, P. & Matin, A. *Escherichia coli* biofilms formed under low-shear modeled microgravity in a ground-based system. *Appl. Environ. Microbiol.* **72**, 7701–7710 (2006).
81. Wilson, J. W. et al. Space flight alters bacterial gene expression and virulence and reveals a role for global regulator Hfq. *Proc. Natl. Acad. Sci. USA* **104**, 16299–16304 (2007).

82. Lomax, B. A. et al. Predicting the efficiency of oxygen-evolving electrolysis on the Moon and Mars. *Nat. Commun.* **13**, 583 (2022).
83. Kelly, S., Verheyen, C., Cowley, A. & Bogaerts, A. Producing oxygen and fertilizer with the Martian atmosphere by using microwave plasma. *Chemistry* **8**, 2797–2816 (2022).
84. Chen, X. et al. Massive water production from lunar ilmenite through reaction with endogenous hydrogen. *Innovation* **5**, 100690 (2024).
85. Moon, T. S. SynMADE: synthetic microbiota across diverse ecosystems. *Trends Biotechnol.* **40**, 1405–1414 (2022).
86. Moon, T. S. Earth: Extinguishing anthropogenic risks through harmonization. *N. Biotechnol.* **80**, 69–71 (2024).
87. Stoesser, D., Rickman, D. & Wilson, S. Preliminary geological findings on the BP-1 simulant. (2010).

Acknowledgements

This work was funded by the Defense Advanced Research Projects Agency B-SURE program (HR001122S0010) and (HR0011259287). The views, opinions, and/or findings expressed in this study should not be interpreted as representing the official views or policies of the Department of Defense or the U.S. Government.

Author contributions

TSM conceived the research idea, acquired the funding, and initiated the study. HL, JD, TSM, and YJT designed the study. HL, JD, YT, EL, and MS performed cultivation and metabolite analyses. RG and MB conducted growth tests under microgravity conditions. AS, DY, and LR developed the AnMBR system and provided the permeate. All authors wrote and approved the paper.

Competing interests

The authors declare no competing interests.

Additional information

Supplementary information The online version contains supplementary material available at <https://doi.org/10.1038/s41467-025-56088-2>.

Correspondence and requests for materials should be addressed to Jinjin Diao, Yinjie J. Tang or Tae Seok Moon.

Peer review information *Nature Communications* thanks the anonymous reviewer(s) for their contribution to the peer review of this work. A peer review file is available.

Reprints and permissions information is available at <http://www.nature.com/reprints>

Publisher's note Springer Nature remains neutral with regard to jurisdictional claims in published maps and institutional affiliations.

Open Access This article is licensed under a Creative Commons Attribution-NonCommercial-NoDerivatives 4.0 International License, which permits any non-commercial use, sharing, distribution and reproduction in any medium or format, as long as you give appropriate credit to the original author(s) and the source, provide a link to the Creative Commons licence, and indicate if you modified the licensed material. You do not have permission under this licence to share adapted material derived from this article or parts of it. The images or other third party material in this article are included in the article's Creative Commons licence, unless indicated otherwise in a credit line to the material. If material is not included in the article's Creative Commons licence and your intended use is not permitted by statutory regulation or exceeds the permitted use, you will need to obtain permission directly from the copyright holder. To view a copy of this licence, visit <http://creativecommons.org/licenses/by-nc-nd/4.0/>.

© The Author(s) 2025